

Patrick Richard, Jean-Paul Troadec, Luc Oger[†]
*Groupe Matière Condensée et Matériaux, UMR CNRS 6626,
 Université de Rennes I, 35042 Rennes Cedex, France*

Annie Gervois
*Service de Physique Théorique, Direction des Sciences de la Matière,
 CEA/Saclay, 91191 Gif-sur-Yvette Cedex, France*

(Dated: November 13, 2000)

We study the effect of the anisotropy of the cells on the topological properties of monodisperse 2D and 3D froths. These froths are built by Voronoï tessellation of actual assemblies of monosize disks (2D) and of many numerical packings of monosize disks (2D) and spheres (3D). We show that topological properties of these froths depend universally on the anisotropy of the cells.

PACS numbers: 87.80.Pa, 82.70.Rr, 61.43.Bn

The physics of disordered froths is of great interest because of their importance in metallurgy (grain aggregates), biology (cells), geology (fracture patterns) etc. . . Such structures can be represented in a simplified way by convex polyhedra filling space (3D froths) or by convex polygons covering the plane (2D froths) which can be obtained by the Voronoï tessellation of packings of equal spheres [1, 2] or disks [3]. It has been shown that these artificial froths behave, from a topological and a metric point of view, like natural froths [2]. In this paper we present new results on the correlation between the anisotropy of the cells and the topological properties of monodisperse 2D and 3D froths issued from monosize packings of disks and spheres.

In order to build our packings of particles, we use five algorithms that have been already described in previous papers as mentioned later. Here, we just recall briefly their principles in three dimensions. They can be divided into three classes.

1. Sequential algorithms

For these algorithms, the particles are placed once at the time. The most simple algorithm of this class is the Random Sequential Adsorption (RSA) [4, 5]. Spheres are deposited at random positions; if the last deposited particle overlaps any of those already present it is removed, otherwise it is permanently fixed. We also use the Modified Random Sequential Adsorption algorithm [6] (MRSA). This algorithm, based on the RSA, allows particles overlapping one or several particles already present to make small displacements to eliminate these overlaps.

The next two sequential algorithms build packings

under the influence of a directional force like the gravity. The first one, the Visscher and Bolsterli's algorithm [7] consists in launching randomly particles at the top of box which contains the packing. A particle is definitively deposited when it is in a stable position, i.e. in contact with 3 particles already placed. The second one is the Powell's algorithm [8], which is very similar to the previous one. It consists in adding spheres, at the lowest position, in contact with 3 randomly chosen spheres already placed.

2. Cooperative algorithms.

We use the Jullien algorithm [1], which is based on the Jodrey-Tory construction [9]. It consists in slowly reducing overlaps of packing of growing soft spheres.

3. Dynamic algorithms

The last algorithm we use is a classical hard sphere molecular dynamic algorithm (event-driven) [10].

According to these algorithms we can build packings of any packing fraction, C , between 0 and 0.74 (FCC packing fraction). The packings are made of approximately 16000 spheres. For the packings of disks we use 2D versions of the algorithms mentioned above. The packings of disks can then have any packing fraction between 0 and 0.907 (triangular lattice). The numerical packings contain approximately 10000 disks. We also use actual packings of disks built on an air table [11]. Such packings are then studied by numerical image analysis. The statistics are made on approximately 3000 disks.

Now, we build our froths and for that purpose we focus

on the Voronoi tessellation of packings of monosize disks and of packings of monosize spheres. We recall that a Voronoi cell is defined as the ensemble of points closer to a given sphere (or disk) than to any other and is characteristic of the local environment around this particle. We have represented in figure 1 an example of

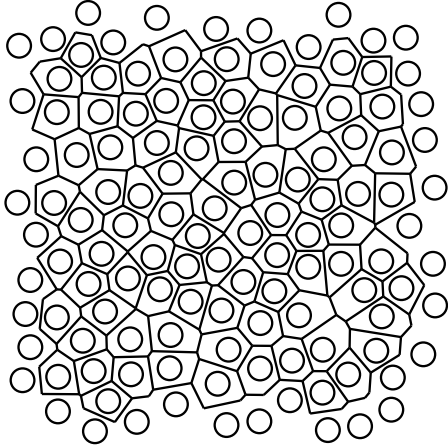


FIG. 1: Example of a 2D Voronoi tessellation. Each cell is a convex polygon. The set of cells fills the plane.

a Voronoi tessellation of a packing of disks.

In 2D, the topological properties of a cell are linked to its number of edges n . Due to the Euler's relation, the mean value of edges per cell, $\langle n \rangle$ is a constant equal to 6. Thus, the topological energy of a 2D froth can be defined as the variance of n : $\mu_2(n) = \langle n^2 \rangle - \langle n \rangle^2$. Metric characteristics of such 2D froths are the mean area $\langle a \rangle$, the mean perimeter of the cells $\langle l \rangle$ and any higher moments of these quantities.

For 3D froths, things are a little more complicated: as the mean number of faces $\langle f \rangle$ is not a constant[2], we have to consider both this mean number and the variance of f , $\mu_2(f) = \langle f^2 \rangle - \langle f \rangle^2$. As for 2D froths, we can compute the mean volume $\langle V \rangle$, area $\langle A \rangle$ and perimeter $\langle L \rangle$ of the cells and any higher moment of these quantities.

We have plotted in figure 2 the evolution of $\langle f \rangle$ versus the packing fraction for the different algorithms used. We observe that this quantity depends not only on the packing fraction but also on the algorithm used, i.e. on the history of the packing. So the packing fraction is clearly not a good quantity in order to describe the state of a froth and we now look for a better parameter. We can turn to the relation between $\langle f \rangle$ and the anisotropy of the cells. This can be done qualitatively by looking at the figure 2. First, we can compare the different algorithms for a given packing fraction. Second, for a given algorithm, (for which we can modify the packing

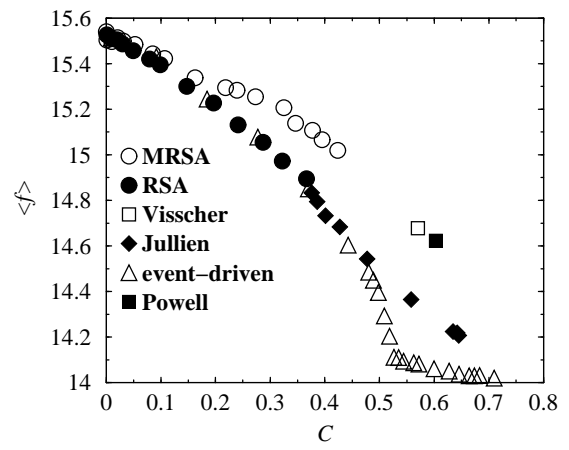


FIG. 2: Evolution of the mean number of faces versus the packing fraction, C , for different algorithms.

fraction) we observe a decrease of $\langle f \rangle$ when the packing fraction increases; actually, it may be checked that cells become more isotropic with this increase.

For example, due to its principle of construction, the MRSA algorithm provides very distorted cells. The Visscher-Bolsterli and Powell algorithms also give anisotropic cells since the direction of the gravity is favored. The last example is event-driven algorithm: for high packing fractions ($C > 0.545$) the system crystallizes [10]; the cells are then more isotropic than those of disordered packings at the same packing fraction. We observe in figure 2 that the higher the anisotropy, the higher the value of $\langle f \rangle$. This result is in agreement with a theory developed by Rivier [12].

In order to study more quantitatively the anisotropy of the cells we have computed for each packing a sphericity coefficient of the cells which we define by

$$K_{sph} = 36\pi \langle V^2 \rangle / \langle A^3 \rangle. \quad (1)$$

For a sphere, this coefficient is equal to 1. For a convex polyhedron, the more anisotropic the polyhedron, the lower K_{sph} . We have reported in figure 3a the variation of $\langle f \rangle$ versus this coefficient. In agreement with Rivier's theory and with our previous qualitative study, we find that the higher the anisotropy the higher $\langle f \rangle$. Furthermore, surprisingly, it seems that all points are positioned on a unique curve. We have also represented, in figure 3b, the evolution of the variance of f , $\mu_2(f)$, with the sphericity coefficient and find once more a unique curve for all the algorithms used. So, unlike packing fraction (see figure 2), the sphericity coefficient seems to be a good parameter in order to describe the 3D froths: all the algorithms used give similar results for a given anisotropy. Then, we have checked if a similar law can be found

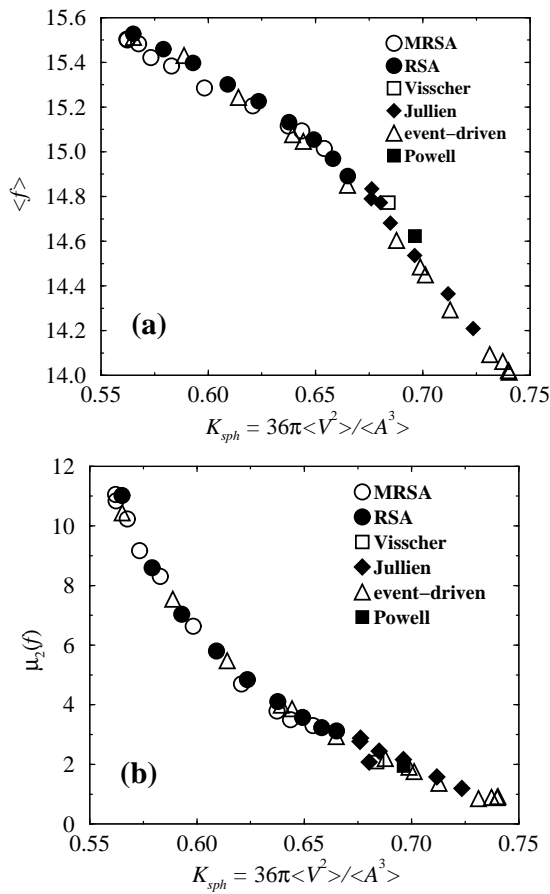


FIG. 3: Evolution of the mean number of faces (a) and of the variance of the number of faces (b) versus the sphericity coefficient K_{sph} for all the algorithms used.

for 2D froths. We first define the 2D equivalent of the sphericity coefficient for 2D froths

$$K_{circ} = 4\pi \langle a \rangle / \langle l^2 \rangle. \quad (2)$$

We have reported in figure 4 the evolution of $\mu_2(n)$ for all packings of disks used versus the coefficient K_{circ} . All the points seems to be in the same curve. As in 3D, the different froths give similar results for a given anisotropy. We can also notice that this curve is linear except on a very short range of packing fraction, where the packings of disks are crystallized ($C > 0.89$) and $\mu_2(n) \approx 0$.

In conclusion we have reported, in this letter, studies on the effect of the anisotropy of cells of disordered 2D and 3D froths on their topological properties. In order to build our froths we use the Voronoi tessellation of packings of monosize particles built by numerical simulation. For the 2D froths, we also use actual packings built on an air table. For 3D froths, we have

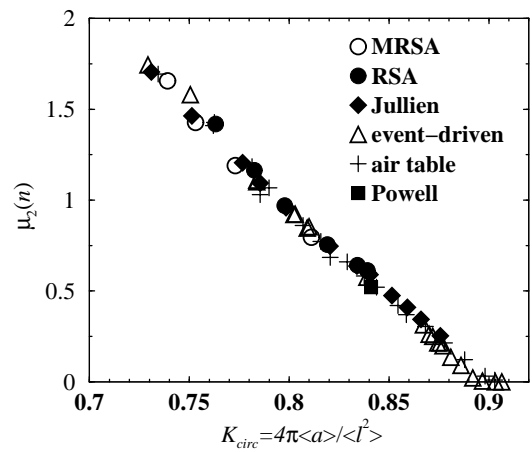


FIG. 4: Evolution of the variance of the number of edges of the cells versus the coefficient K_{circ} , for froths generated from 2D disk packings.

shown, in agreement with Rivier's theory that the mean number of faces $\langle f \rangle$ increases when the anisotropy of the cells increases. A more careful study shows that this quantity and the variance of the number of faces $\mu_2(f)$ seem to depend universally on this anisotropy. A similar result exists in 2D.

An open question is the following: is that universality verified by natural froths like, for example, polycrystals? The answer is difficult because it is not easy to measure the mean quantities in the expression of K_{sph} . The next step of this work is to study the link between the anisotropy of the 3D froths and the anisotropy of their cuts (see [13] for a preliminary work on cuts of 3D froths). We expect to find information on the 3D structure from the cuts.

[†] Electronic address: luc.oger@univ-rennes1.fr

- [1] R. Jullien, P. Jund, D. Caprion, and D. Quitman. Computer investigation of long range correlations and local order in random packings of spheres. *Physical Review E*, 54:6035–6041, 1996.
- [2] L. Oger, A. Gervois, J.-P. Troadec, and N. Rivier. Voronoi tessellation of packings of spheres: topological correlation and statistics. *Philosophical Magazine B*, 47:177–197, 1996.
- [3] J. Lemaitre, A. Gervois, J.-P. Troadec, N. Rivier, M. Ammi, L. Oger, and D. Bideau. Arrangement of cells in Voronoi tessellations of monosize packing of discs. *Philosophical Magazine B*, 67(3):347–362, 1993.
- [4] B. Widom. Random sequential addition of hard spheres to a volume. *The Journal of Chemical Physics*, 4:3888–3894, 1966.
- [5] E. L. Hinrichsen, J. Feder, and T. Jossang. Geom-

- etry of random sequential adsorption. *Journal of Statistical Physics*, 44:793–827, 1986.
- [6] R. Jullien and P. Meakin. Random sequential adsorption with restructuring in two dimensions. *Journal of Physics A: Math. Gen.*, 25:L189–L194, 1992.
- [7] W.M. Visscher and M. Bolsterli. Random packing of equal and unequal spheres in two and three dimensions. *Nature*, 239:504–507, 1972.
- [8] M.J. Powell. Computer-simulated random packing of spheres. *Powder Technology*, 25:45–52, 1980.
- [9] W.S. Jodrey and E.M. Tory. Computer simulation of close random packing of equal spheres. *Physical Review A.*, 32:2347–2351, 1985.
- [10] P. Richard, L. Oger, J.-P. Troadec, and A. Gervois. Geometrical characterization of hard sphere systems. *Physical Review E*, 60:4551–4558, 1999.
- [11] J. Lemaitre, A. Gervois, H. Peerhossaini, D. Bideau, and J.P. Troadec. An air table designed to study two-dimensional disc packings: preliminary tests and first results. *Journal of Physics D: Applied Physics*, 23:1396–1404, 1990.
- [12] N. Rivier. Recent results on the ideal structure of glasses. *Journal de Physique Colloque*, C9:91–95, 1982.
- [13] L. Oger, P. Richard, J.-P. Troadec, and A. Gervois. Comparison of two representations of a random cut of identical sphere packing. *The European Journal of Physics B*, 14:403–406, 2000.